Željko Domazet[1], *Francisko Lukša*[1], *Miro Bugarin*[1]

Failure of two overhead crane shafts

[1]Faculty of Electrical Engineering, Mechanical Engineering and Naval Architecture; University of Split; Split, Croatia

Abstract

The failure analysis of two overhead crane shafts is presented: the failure of an overhead crane drive shaft and the failure of an overhead crane gearbox shaft, due to rotating-bending fatigue. The fracture of the overhead crane drive shaft originated in small radius fillet between two different diameters of the shaft. A new shaft was made with a larger-size fillet, resulting in reduced stress concentration in this region. The failure of the overhead crane gearbox shaft originated in the intersection of two stress raisers, due to a change in the shaft diameter and in the keyway corner. A new shaft was made with a larger-size fillet and a larger size radius of the keyway corner to minimize stress concentration in this section. In both cases the installed couplings were replaced by gear couplings in order to allow parallel and angular misalignment as well as to avoid additional load due to misalignment. The analysis shows that the fatigue life can be significantly increased with a simple change in the structural details

Keywords: *Failure analysis; Shaft failures; Overhead cranes*

1. Introduction

The fatigue fractures of shafts originate at points of stress concentration, such as changes in the shaft diameter and ends of the keyways. The sharp corner at the intersection between two different diameters of the shafts or in the bottom of the keyway can cause local stress to be few times greater than the average nominal stress. The failure analysis of an overhead crane trolley drive shaft is presented in the first part of this paper. The failure originated in the radius fillet between two different diameters of the shaft. The failure analysis of an overhead crane trolley gearbox shaft is presented in the second part of the paper. The failure of this shaft originated at the intersection of two stress raisers, the change in the shaft diameter and keyway.

2. Failure of overhead crane drive shaft

In "Steelworks Split" the high-speed electric overhead crane, Fig.1, was suitable for transport of the billets from the melt shop to the rolling mill hall. The crane was rated at 10 tons with a span of 20.5 m and handled about 100 lifts and transports per day, each lift averaging 5 tons. The stepped drive shaft used for an overhead crane trolley wheel fractured after 24 months of service. The electric motor power rating was 3 kW with an output speed of 940 rpm. The maximum travel speed of the trolley was 32 m/min.

The shaft was connected with the gearbox by a roller chain coupling, supported by two roller bearings and connected with the wheel by a key, Figure 2.

The shaft was made of quenched and tempered steel 25CrMo4 according to German standard DIN (Deutsches

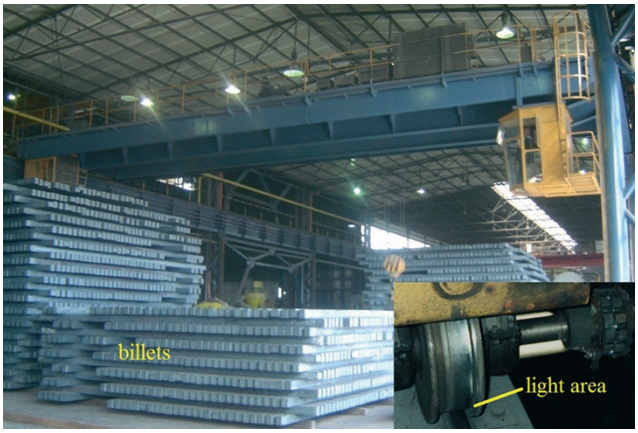

Fig. 1. Overhead crane for transport of billets

Institut für Normung) [1]. The chemical composition of material was verified by using quantometer. The hardness and the microstructure were confirmed to be tempered steel 25CrMo4. The fracture occurred on the fillet

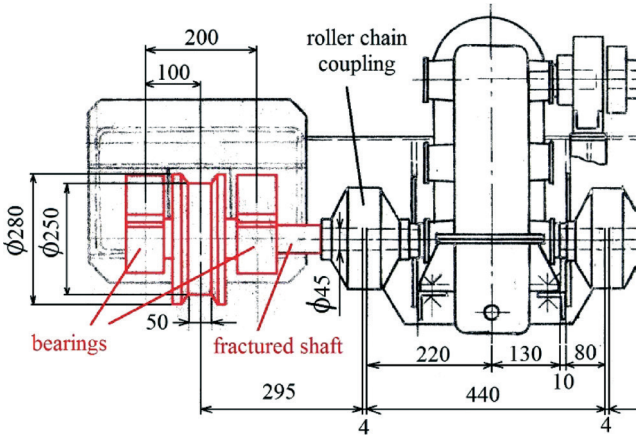

Fig. 2. Overhead crane trolley [2]

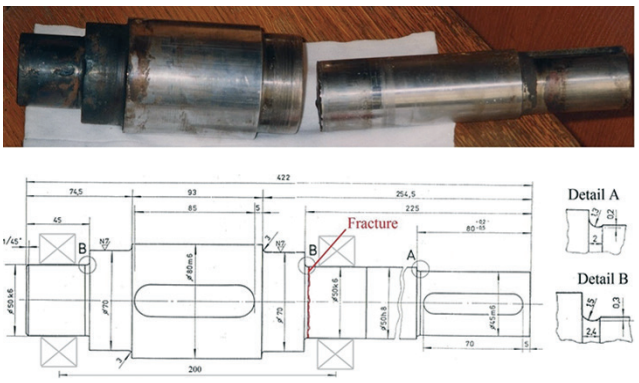

Fig. 3. Stepped drive shaft

due to change between two different diameters of the shaft approximately 225 mm from the driven end and approximately 30 mm from one end of the keyway where the crane wheel was keyed to the axle, Figure 3.

2.1. Fracture surface investigation

The contour of the fracture surface was convex with respect to the smaller-section side. There were three fracture regions, Figure 4: a region of multiple crack origins around the outer perimeter (at A); a region of the crack propagation zone (at B); and a region of the final, fast fracture (at C).

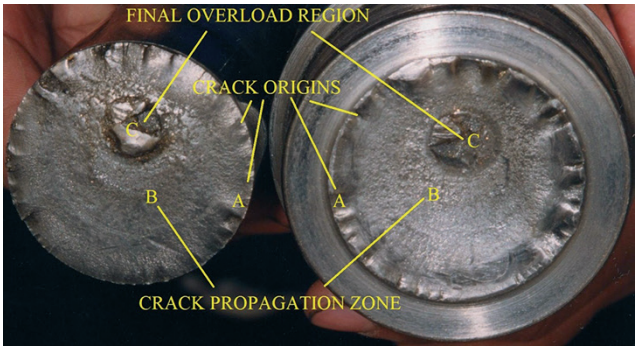

Fig. 4. Fracture surfaces

The presence of multiple crack origins separated by ratchet marks around the outer perimeter was an indication of rotational-bending fatigue with severe stress concentration.

The relatively small size of the final fracture region was an indication of low nominal stress. In rotational-bending, during each revolution, every point of the shaft circumference was subjected to tensile-compressive stress and therefore the crack could be initiated at any point on the shaft periphery.

The individual cracks propagated toward a single crack front, region B, Figure 4. The crack surfaces were pressed together during the compressive component of the stress cycle, and mutual rubbing occurred. The beach marks were not visible because they were obliterated by rubbing.

The conclusion from the surface investigation was that the shaft fractured as a result of rotational-bending fatigue. The primary cause of the fracture was the bending load during the rotation, although the total load was a combination of bending and torsional loads. The small radius of the fillet at a change in shaft diameter, detail B in Figure 3, resulted in high stress concentration, which initiated the crack.

The visual examination of the wheel and rail revealed smooth and light contact area on the sides of both parts due to mutual rubbing, detail in Figure 1, which was caused by additional torsional load. Post-failure verification of parallelism and straightness of the rails with optical instrument revealed misalignment in parallelism and straightness.

2.2. Stress analysis

2.2.1. Bending stresses

During normal operation, bending stresses in the critical area were caused by a wheel vertical load. The wheel vertical load was considered as a force applied at the center line of the wheel contact with the shaft, see Figure 5. The applied force was calculated from the design load, see reference [2].

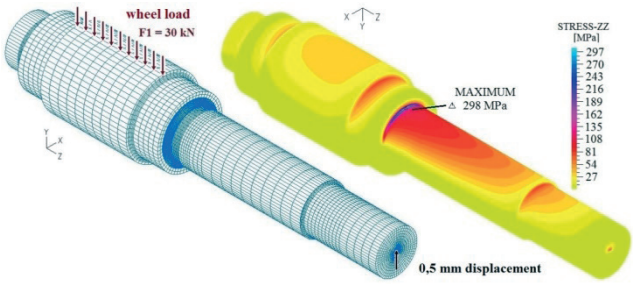

Fig. 5. Numerical analysis

A numerical analysis of local stresses was done by the finite element method using ADINA software. The linear elastic model with 3D solid elements with eight DOF per nodes was used, Figure 5. Each node had 3 degrees of freedom, translation in X, Y and Z direction. The model is fixed in the line on the positions of bearing centers and loaded with concentrated forces in the nodes. The numerical analysis of local stresses revealed that design force due to vertical load should not have led to shaft fracture. Force 30 kN caused local stresses of 79 MPa in the critical area.

Post-failure verification revealed parallel misalignment of 0.5 mm between two shaft axes. The numerical analysis of local stresses revealed that displacement of 0.5 mm caused an increase in local stresses in the critical area three times (298 MPa), Figure 5.

A roller chain coupling was used to transmit power between shafts. The torque was transmitted through a double roller chain. Due to clearances between the chain and the sprocket teeth on two couplings, the roller chain coupling permitted eccentricity – ε (parallel misalignment) between shafts up to 2% of the roller chain pitch

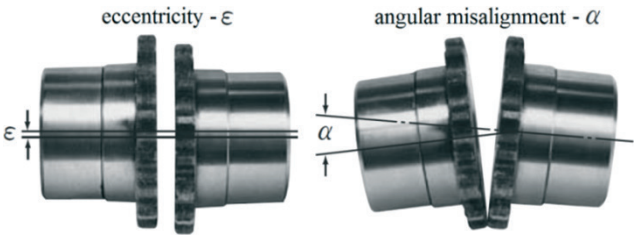

Fig. 6. Roller chain coupling [3]

and angular misalignment – α between shafts up to 1°, [3], see Figure 6.

If eccentricity and angular misalignment between the wheel shaft axis and the drive axis is higher than the chain coupling can compensate, there is a vertical force on the end of the wheel shaft and also corresponding additional bending stresses in the critical place.

2.2.2. Torsional stresses

The maximum applied torque of 716 Nm in the drive shaft was estimated from the electric motor power rating of 3 kW, the maximum travel speed of the trolley of 32 m/min and the wheel diameter was 250 mm. The calculated nominal shear stress for the shaft diameter of 50 mm was 28.6 MPa. The stress concentration factor due to torsional stress at a change of the shaft diameter according to literature [4] was 1.8. The maximum shear local stress at the intersection of the change of the shaft diameter due to stress concentration was 51.5 MPa.

From the comparison between bending and shear stresses it was concluded that bending stresses were dominant for the shaft fracture.

2.3. Corrective action

A corrective action was considered in two ways:

a) Decreasing the stress concentration in the critical area by increasing the size of the fillet radius and

b) Reducing the influence of parallel misalignment between the shaft axis and coupling axis on local stresses by changing the type of the coupling, which permitted more parallel misalignment between axes.

2.3.1. Increasing the size of the fillet radius

The distance between the large diameter of the shaft (wheel) and the bearing was 11 mm, Figure 7. The spacer was positioned between the wheel and bearing. Increasing the size of the fillet radius was limited by the design of the spacer.

Therefore, numerical experiments were carried out for four different sizes of the fillet radius in order to reduce local stresses below the endurance limit, Figures 8 and 10.

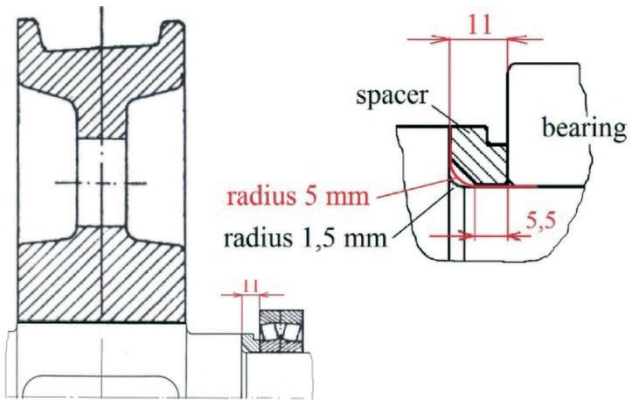

Fig. 7. Design of the spacer

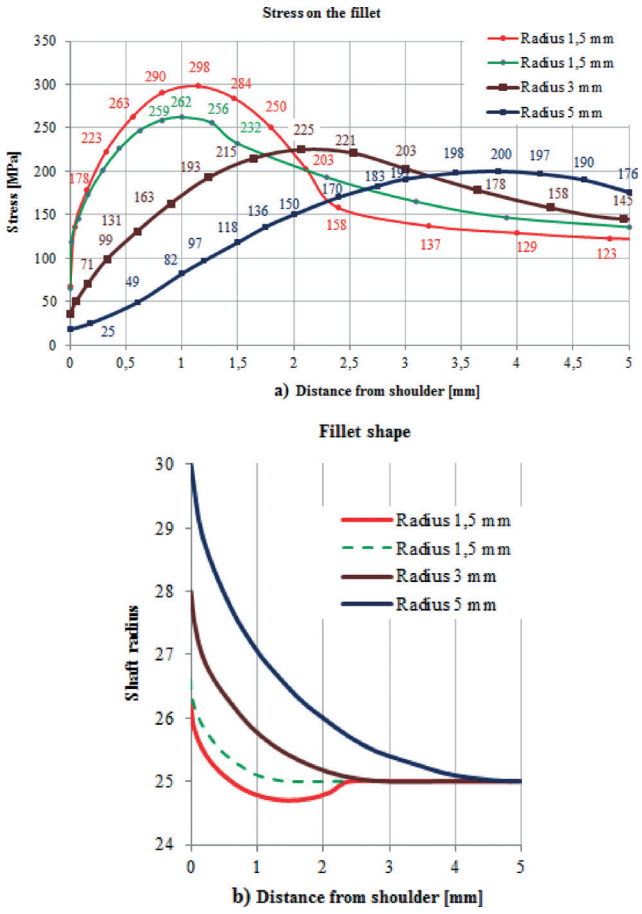

Fig. 8. Stress distribution

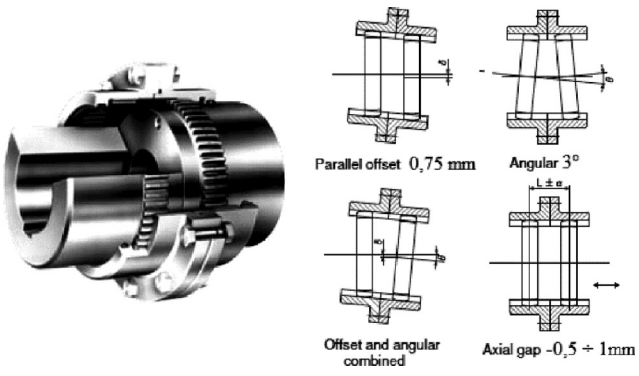

Fig. 9. Gear coupling, [7]

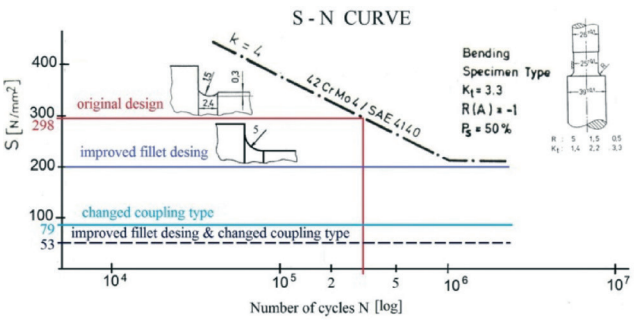

Fig. 10. Influence of corrective actions on fatigue life

The stress concentration factors in the critical areas had a good agreement with literature [4] and [5]. The fatigue strength curve of the material was used from literature [6].

The curves in Figure 8 show the increasing size of the fillet radius from 1.5 mm to 5 mm, reducing maximum local stress by about 1.5 times (from 298 to 200 MPa).

2.3.2. Change of the coupling type

A gear coupling was considered to substitute the roller chain coupling, Figure 9. The gear coupling can accommodate more eccentricity and angular misalignment than the roller chain coupling. According to [7], the gear coupling permits parallel offset 0.75 mm, angular 3° and axial gap from -0.5 to 1 mm. Since post-failure verification revealed parallel misalignment of 0.5 mm between two shaft axes, the application of the gear coupling in this case can eliminate force on the shaft due to misalignment and can also reduce local stresses in the critical area.

Figure 10 shows the influence of considered corrective actions on fatigue life.

The actual service life was estimated from the working time of the crane, the number of liftings and the wheel diameter. The crane was in service for about 400 working days in the period of two years. The average number of transports per day was 100 with the travel of the trolley 10 m per each transport. For the wheel diameter of 250 mm and the corresponding shaft the actual service life was about $4.8 \cdot 10^5$ cycles. The estimated service life from the numerical model was about $3 \cdot 10^5$ cycles, Figure 10.

The redesign of the shaft fillet radius from 1.5 mm to 5 mm reduced maximum local stress below the fatigue endurance limit (about 90% of endurance limit). The application of a gear coupling to accommodate parallel misalignment reduced maximum local stress to about 35% of the endurance limit, what was more than two times in comparison to the redesign of the shaft fillet radius. A combination of the fillet radius redesign and the application of the gear coupling additionally reduced local stresses, Figure 10.

Based on this analysis, the actual service life of the shaft can be improved from the finite (about $4.8 \cdot 10^5$ cycles) to the infinite lifetime.

2.3.3. Correction

New shafts were made from quenched and tempered steel 42CrMo4 according to DIN [1] with a larger-size fillet, which minimized stress concentration in this region and prevented recurrence of the failure. The roller chain couplings were replaced by gear couplings to reduce the influence of parallel misalignment between the shaft axis and coupling axis on local stresses.

3. Failure of overhead crane gearbox shaft

An electric overhead crane, Fig. 11, was suitable for the transport of a ladle with liquid steel from the ladle furnace to the continuous casting machine. The crane was rated at 50 tons with a span of 18.4 m and handled about 20 lifts and transports per day, each lift averaging 43 tons. The stepped drive shaft used in an overhead crane trolley gearbox, Figure 12, broke after 36 months of service.

The electric motor power rating was 5.5 kW with an output speed of 940 rpm. The maximum travel speed of the trolley was 20 m/min. The overhead crane trolley gearbox [8] is shown in Figure 12 and the shaft is shown in Figures 13 and 14.

Fig. 11. Overhead crane for transport of ladle with liquid steel

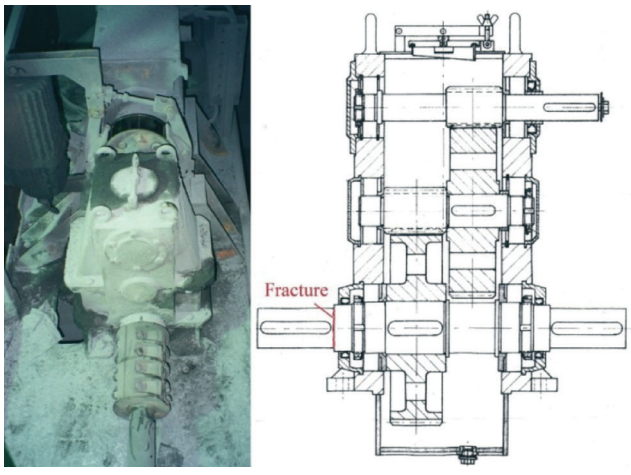

Fig. 12. Overhead crane trolley gearbox

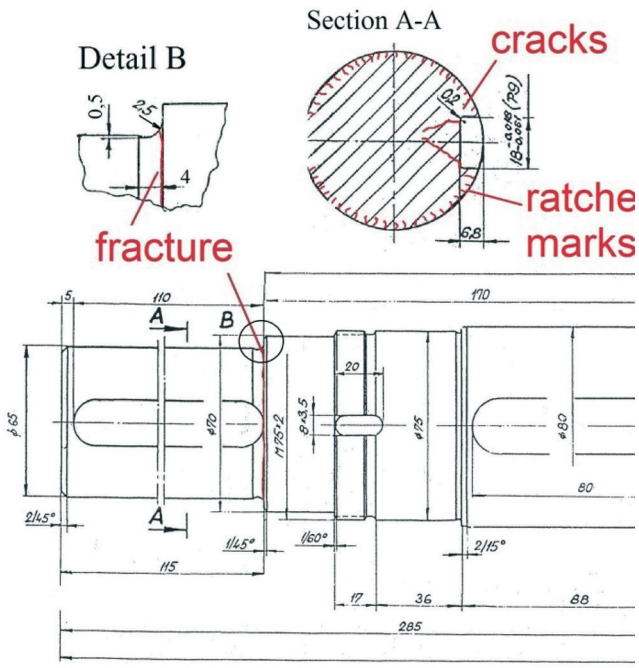

Fig. 13. Stepped drive shaft [8]

Fig. 14. Stepped drive broken shaft

3.1. Fracture surface investigation

The shaft was made of construction steel St 52-3 according to DIN [9]. The fracture occurred on a fillet due to change between two different diameters of the shaft approximately 110 mm from one end. The contour of the fracture surface was convex with respect to the smaller-section side.

There were four fracture regions, Figure 15. Numerous ratchet marks (at A), on the outer edge of the surface and the dark band at this edge indicate fatigue cracks initiation, what is a characteristic of rotational-bending fatigue. Two cracks (at B) from the keyway corners suggested torsional stresses. The cracks propagated circumferentially around the shaft (at C). The final fracture was a mixed ductile and brittle fracture in the middle of the elliptical contour (at D). The beach marks were not visible because they were obliterated by rubbing.

In this case there were two stress raisers in the same area: a sharp corner in the keyway and a change in the shaft diameter. Additionally, the end of the keyway was due to change in the shaft diameter, fracture section in Figure 13, causing high concentration of stresses.

The conclusion from the surface investigation was that the shaft fractured as a result of the rotational-bending fatigue due to high stress concentration. The cracks were initiated

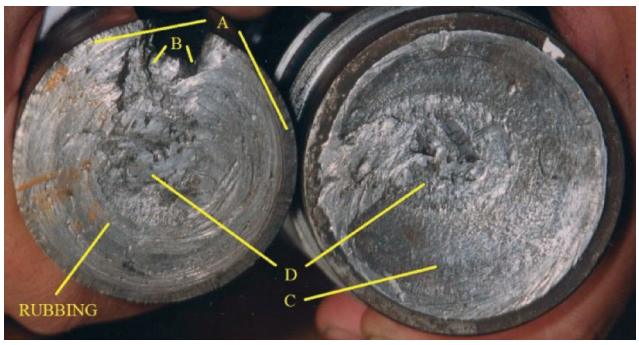

Fig. 15. Fracture surfaces

in the intersection of two stress raisers, on the sharp corner in the keyway and on the radius of the fillet due to change in the shaft diameter, detail B in Figure 13.

3.2. Stress analysis

3.2.1. Bending stresses

A split muff coupling was used to transmit power between the shafts, Fig.12.

The split muff coupling is a type of rigid coupling and should be used when the alignment of the two shafts can be maintained very accurately. A small missalignment between two shafts can cause high stresses. Post-failure verification revealed parallel misalignment of 0.8 mm between the gearbox shaft axis and the drive shaft axis of the wheel, Figure 16.

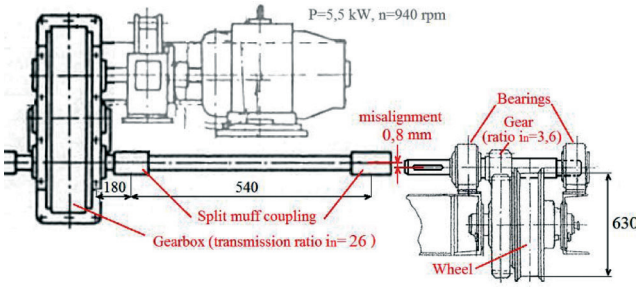

Fig. 16. Misalignment between the gearbox shaft axis and drive shaft axis of the wheel

The numerical analysis of local stresses was done by the finite element method using ADINA software. The applied force of F=15000 N was estimated from the parallel misalignment of d=0.8 mm according to expression (1), Figure 17, where l = 720 mm and a = 180 mm, Figure 16.

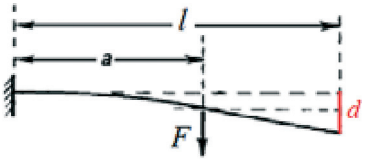

Fig. 17. Deflection

$$d = \frac{Fa^2}{6EI}(3l - a) \quad (1)$$

The linear elastic model with 3D solid elements with eight DOF per nodes was used, Figure 18. Each node had 3 degrees of freedom, translation in X, Y and Z direction. The model is fixed in the back side face and loaded with concentrated forces in the node on the front side.

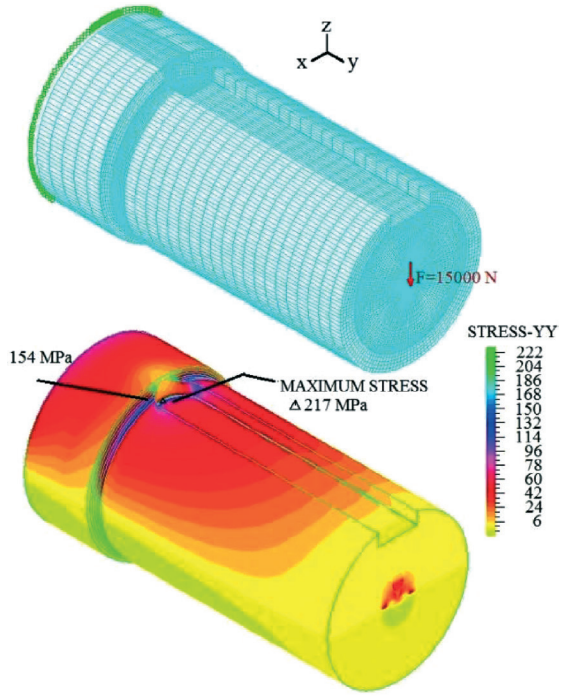

Fig. 18. Numerical analysis

The FEM analysis of local stresses revealed that the maximum stress 217 MPa was in the sharp corner of the keyway and the stress on the fillet due to change in the shaft diameter near the keyway was 154 MPa, Figure 18. Stress concentration factors in critical areas had a good agreement with literature [4] and [5].

3.2.2. Torsional stresses

The maximum applied torque of 1458 Nm in the gearbox output shaft was estimated from the electric motor power rating of 5.5 kW with an output speed of 940 rpm and the gearbox transmission ratio 26. The calculated shear stress for the shaft diameter of 65 mm was 26.5 MPa. The stress concentration factor due to torsional stress due to change of the shaft diameter was 1.5 and due to the keyway it was 1.7 [4]. The maximum local stress due to change in the shaft diameter and the keyway due to stress concentration was 67.6 MPa.

3.3. Corrective action

Corrective action were considered in both critical areas:

a) Increasing the fillet radius due to change in the shaft diameter from 2.5 mm to 4 mm, Fig. 19.

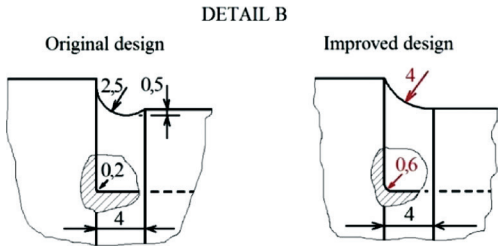

Fig. 19. Original and improved design of the fillet radius

b) Increasing the radius in the keyway corner of the maximum size. The maximum radius size in the keyway corner for the shaft diameter 65 mm according to DIN [10] was 0.6 mm, Fig. 19.

c) Reducing the influence of parallel misalignment between the shaft axis and coupling axis on local stresses by changing the type of coupling which permits parallel misalignment between axes.

3.3.1. Increasing both the radius in the keyway corner and the radius due to change in the shaft diameter.

The FEM analysis of local stresses after the redesign revealed decreasing the maximum bending stress in the sharp corner of the keyway from 217 MPa to 145 MPa as well as decreasing stresses of the fillet radius due to change in the shaft diameter from 154 MPa to 86 MPa, Figure 20.

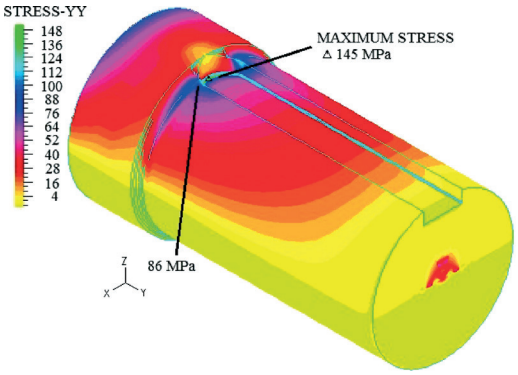

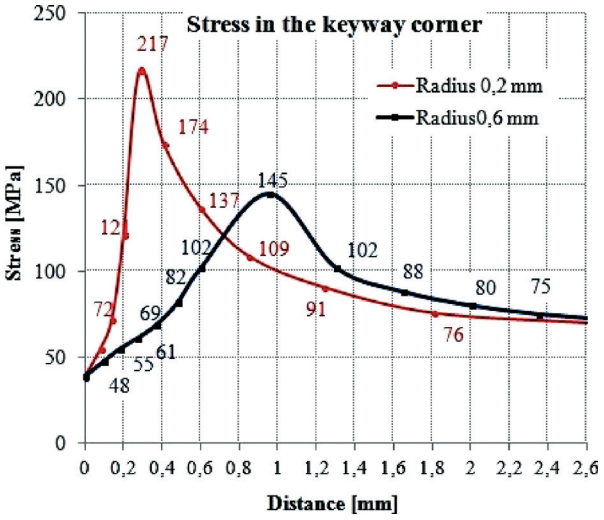

Fig. 20. Numerical analysis

3.3.2. Change of the coupling type

A gear coupling was considered to substitute the split muff coupling since post-failure verification revealed parallel misalignment of 0,8 mm between two shaft axes. The application of gear couplings can eliminate force on the shaft due to misalignment and can also reduce local stresses on the critical area.

Figure 21 shows the influence of considered corrective actions on the fatigue life. The fatigue strength curve of the material is used from literature [11].

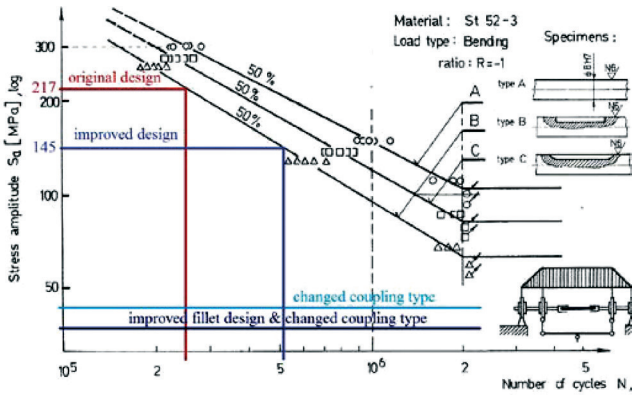

Fig. 21. Influence of corrective actions on the fatigue life

The actual service life was estimated from the working time of the crane, the number of liftings and the wheel diameter. The crane was in service for about 800 working days during a three year period. The average number of transports per day was 20 with the travel of the trolley 12 m per each transport. For the wheel diameter of 630 mm and the corresponding shaft, the actual service life was $3.5 \cdot 10^5$ cycles. The estimated service life from the numerical model was about $3 \cdot 10^5$ cycles, Figure 10.

The redesign of the shaft fillet radius reduced the maximum local stress and the estimated fatigue life was about two times longer according to actual fatigue life, Figure 21. The application of a gear coupling to accommodate parallel misalignment eliminated force due to misalignment, and bending stresses became negligible. A combination of the fillet radius redesign and application of the gear coupling additionally improved fatigue life.

Based on this analysis, the actual service life of a shaft can be improved from finite ($3.5 \cdot 10^5$ cycles) to infinite lifetime.

3.3.3. Correction

New shafts were made with the radius size due to change in the shaft diameter 4 mm and the radius size in the keyway corner 0.6 mm, minimizing stress concentration in both critical areas and preventing recurrence of the failure.

Split muff couplings were replaced by gear couplings to reduce the influence of parallel misalignment between the shaft axis and the coupling axis on local stresses.

4. Conclusion

The failure analysis of two overhead crane shafts showed that the overhead crane drive shaft and the gearbox shaft fractured as a result of rotational-bending fatigue. In both cases the fracture occurred on the places with high stress concentration. The fracture of the overhead crane drive shaft originated in the small radius fillet between two different diameters of the shaft. The fracture of the overhead crane gearbox shaft was initiated in the intersection of two stress raisers on the sharp corner in the keyway and on the radius of the fillet due to change in the shaft diameter. The failure analysis revealed that the design load should not have led to shaft fracture and that there also existed additional load unforeseen by the design. The post-failure verification in both cases revealed parallel misalignment between two shaft axes. Corrective actions were considered in two ways: to improve service life by a small change in the design and to remove the unforeseen additional load due to misalignment between two shaft axes.

In the case of the overhead crane drive shaft, increasing the size of the fillet radius from 1.5 mm to 5 mm decreased the maximum local stress below the endurance limit, resulting in significant increasing of the fatigue life. In the case of the overhead crane gearbox shaft, increasing the radius size due to change in the shaft diameter from 2.5 mm to 4 mm and the increasing of the radius size in the keyway corner from 0.2 to 0.6 mm extends the fatigue life more than twice. The gear coupling, compared to the roller chain coupling and especially to split muff coupling, allows more angular and parallel misalignment, prolonging significantly shaft service life. Based on this analysis, the actual service life of the shaft can be improved from finite to infinite lifetime.

References

[1] Deutsches Institut für Normung. DIN 17200, 1987 (DIN, Berlin)

[2] Crane design and manual book of billet overhead crane in "Steelworks Split"

[3] D.I.D., "Power transmission & conveyor chain", catalog, Daido Kogyo co, Kumasaka-Cho, Kaga-City, Ishikawa Pref, 922-8686, Japan, 2007.

[4] W.D. Pilkey, D.F. Pilkey, "Stress concentration factors", 3rd ed., Hoboken, John Wiley & Sons, New York, 2008.

[5] E. Heibach, "Betriebfestigkeit", VDI Verlag Gmbh, Düsseldorf, 1989.

[6] V. Grubišić, G. Jacoby, "Fracture analysis, validation and technologies to increase the strength of materials", Seminar, Firenze, March 1995.

[7] SEISA, "Gear coupling", catalog, Seisa Gear Ltd., Kaizuka, Osaka, Japan, 2011.

[8] Crane design and manual book of ladle overhead crane in "Steelworks Split"

[9] Deutsches Institut für Normung. DIN 17100, 1980 (DIN, Berlin)

[10] Deutsches Institut für Normung. DIN 6885-1, Paßfedern nuten, 1968 (DIN, Berlin)

[11] Ž. Domazet, "Fatigue stress concentration factor for shaft with different keyways in bending ", Osterreichische Ingenieur und Architekten Zeitschrift, 142. Jg., Heft 6/1997